Enhanced Quench Propagation in $Bi_2Sr_2CaCu_2O_x$ and $YBa_2Cu_3O_{7-x}$ Coils via a Nanoscale Doped-Titania-Based Thermally Conducting Electrical Insulator

Sasha Ishmael, *Member, IEEE*, Haojun Luo, Marvis White, Frank Hunte, X. T. Liu, Natalia Mandzy, John F. Muth, *Member, IEEE*, Golsa Naderi, Liyang Ye, *Student Member, IEEE*, Andrew T. Hunt, and Justin Schwartz, *Fellow, IEEE*

***Abstract*—The significant amount of energy stored in a large high-field superconducting magnet can be sufficient to destroy the coil in the event of an unprotected quench. For magnets based on high-temperature superconductors (HTSs), such as $Bi_2Sr_2CaCu_2O_x$ (Bi2212) and $YBa_2Cu_3O_{7-x}$ (YBCO), quench protection is particularly challenging due to slow normal zone propagation. A previous computational study showed that the quench behavior of HTS magnets is significantly improved if the turn-to-turn electrical insulation is thermally conducting, enhancing 3-D normal zone propagation. Here, a new doped-titania electrical insulation with high thermal conductivity is evaluated. The thermal conductivity of the insulation is measured at cryogenic temperatures, and its chemical compatibility with Bi2212 round wires is determined. Thin layers of the insulation are deposited onto the surface of Bi2212 and YBCO wires, which are then wound into small coils to study the quench behavior. Results show that the critical current and homogeneity of Bi2212 coils are improved relative to coils reacted with mullite insulation. Relative to similar coils with conventional insulation (mullite for Bi2212 and Kapton for YBCO), the turn-to-turn quench propagation is increased by a factor of 2.8 in Bi2212 coils at 4.2 K and self-field and by a factor of 2.5 in YBCO coils at 4.2 K and 5 T. These results indicate that doped-titania insulation may significantly improve Bi2212 and YBCO coils. Increased normal zone propagation velocity enhances quench detection and quench protection, and the thinness of the insulation relative to the most common alternatives increases the magnet winding pack current density and reduces the coil specific heat.**

***Index Terms*—$Bi_2Sr_2CaCu_2O_x$, high-temperature superconductor (HTS), insulation, quench detection, quench protection, thermal conductivity, $YBa_2Cu_3O_{7-x}$.**

Manuscript received November 27, 2012; revised March 1, 2013; accepted April 17, 2013. Date of current version August 2, 2013. This work was supported by the Office of High Energy Physics, U.S. Department of Energy (DOE), through a Phase-I and Phase-II Small Business Technology Transfer and from an earlier DOE Small Business Innovation Research. This paper was recommended by Associate Editor L. Chiesa.

S. Ishmael, F. Hunte, X. T. Liu, G. Naderi, L. Ye, and J. Schwartz are with the Department of Materials Science and Engineering, North Carolina State University, Raleigh, NC 27695-7907 USA (e-mail: sishmael@ieee.org).

H. Luo and J. F. Muth are with the Department of Electrical and Computer Engineering, North Carolina State University, Raleigh, NC 27695-7907 USA.

M. White, N. Mandzy, and A. T. Hunt are with nGimat, Lexington, KY 40511 USA.

Color versions of one or more of the figures in this paper are available online at http://ieeexplore.ieee.org.

Digital Object Identifier 10.1109/TASC.2013.2269535

I. Introduction

THE commercial development of high-temperature superconductor (HTS)-based wires and, in particular, $Bi_2Sr_2CaCu_2O_x$ (Bi2212) round wires (RWs) and $YBa_2Cu_3O_{7-x}$ (YBCO) coated conductors (CCs) has progressed such that large-scale magnet development projects are under way. These projects either take advantage of the ability of HTS conductors to carry high transport current density at high magnetic field and low temperature for applications in science (nuclear magnetic resonance and high-energy physics) [1], [2] and energy storage [3], [4] or at relatively low magnetic field and elevated temperature for applications in motors, generators, and fault current limiters [5]–[7].

One of the key remaining challenges preventing rapid advancement of HTS-based magnets is quench protection. It has been repeatedly shown that the minimum quench energy (MQE) of HTS magnets and conductors is significantly larger than in NbTi and Nb_3Sn magnets but that the normal zone propagation velocity (NZPV) is significantly slower, i.e., as much as two orders of magnitude slower [8]–[18]. Thus, although quenching may be significantly less likely to occur, quench detection, and thus quench protection, is significantly more difficult. While there are a number of possible approaches to improve quench protection in HTS magnets, most efforts to increase the NZPV also reduce the MQE. One approach proposed recently is the use of thermally conducting electrical insulation as the turn-to-turn insulation within the magnet. Computational results showed that this approach significantly improves the turn-to-turn NZPV, resulting in a magnet that is more stable (higher MQE) and easier to protect through 3-D growth of the normal zone [19].

Here, we report on a thermally conducting electrical insulator developed specifically for HTS magnets. The insulation, i.e., a doped-titania nanopowder, is produced by a combustion chemical vapor condensation (CCVC) technique. Results reported include measurements of the thermal conductivity at room temperature (RT) and cryogenic temperatures, critical current measurements to determine the chemical compatibility of the insulation with Bi2212, and measurements of the effects of the insulation on transverse quench propagation in Bi2212 and YBCO coils.

TABLE I
SUMMARY OF SAMPLES AND THE MEASUREMENTS PERFORMED

Samples	Insulation	Measurement
Thin films on sapphire substrates	• Large doped-titania with a polyimide matrix • Small doped-titania with a polyimide matrix • Polyimide	3ω thermal conductivity at room temperature, 77 K and 4.2 K
Bi2212 short sample wires (heat treated with insulation; polyimide burns out during heat treatment)	• Doped-titania in polyimide • Doped-titania in polyimide with a polyimide topcoat • Braided mullite fiber • Bare wire	I_c at self-field, 4.2 K
Bi2212 coils (heat treated with insulation; polyimide burns out during heat treatment)	• Doped-titania in polyimide • Doped-titania in polyimide with a polyimide topcoat • Braided mullite fiber	I_c at self-field, 4.2 K Quench behavior at self-field, 4.2 K
YBCO pancake coils	• Large doped-titania with a polyimide matrix • Small doped-titania with a polyimide matrix • Kapton	Quench behavior self-field, 4.2 K and 77 K

II. EXPERIMENTAL APPROACH

Experiments are designed to measure the thermal properties of the insulation materials, their compatibility with superconducting wires, and their impact on quench behavior. The sample types and experiments, described in detail in this section, are summarized in Table I.

A. Sample Preparation

Samples are prepared specifically for each of the measurements to be performed. Thermal conductivity measurements require thin films on highly controlled substrates, compatibility studies require short samples, and quench experiments require multiturn coils. This section summarizes the sample preparation for each of these experiments.

1) Thin Films on Sapphire for Thermal Conductivity: Thin-film samples of the doped titania are prepared on sapphire wafers using the Mayer rod technique at RT [20]. Samples were prepared using two sizes of doped-titania particles mixed in a polyimide matrix; the smaller nanoparticles have diameters less than 20 nm on average, and the larger nanoparticles have diameters ranging from 40 to 60 nm. The film thicknesses are measured using a DekTak3 stylus profilometer; thicknesses range from 5 to 11 μm. A sample of pure polyimide is similarly prepared for comparison.

In the three-omega (3ω) method used for thermal conductivity measurements (described in detail below), a thin electrically conductive metal wire is photolithographically defined on an insulating substrate and serves as a heater and a sensor. Here, a 5-nm Cr adhesion layer and a 200-nm-thick gold film are deposited on the films by e-beam evaporation. Thin heaters (1 and 3 mm long and 10 μm wide) are fabricated on the sample surfaces. Fig. 1 illustrates the heater wire pattern with the four-probe contact pads for making connections.

2) Bi2212 Short Samples and Coils:

Short samples: Bi2212 magnets are typically manufactured via a wind-and-react process and require that the turn-to-turn insulation be incorporated into the winding before heat treatment. Thus, it is essential that the insulation does not adversely affect Bi2212 performance and that it survives the Bi2212 heat treatment process, which typically has a peak processing temperature of about 890 °C in 100% flowing oxygen.

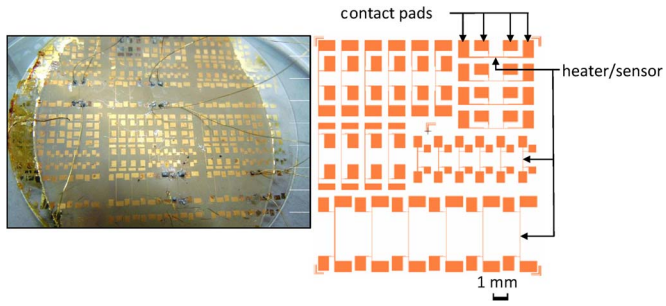

Fig. 1. Schematic of the mask pattern and a photograph of a typical thin-film sample for thermal conductivity measurements; both show the four-point geometry. Multiple locations are patterned to provide measurements at different locations and because some lines become discontinuous due to surface roughness. The sizes of the heaters/sensors are varied so that the pattern resistance can be varied in order to optimize the measurements.

Green Bi2212 RWs from Oxford Superconducting Technology lot identifier PMM091221-3B are coated with insulation at RT and heat treated using a standard Bi2212 heat treatment. The Bi2212 wire is 0.8 mm in diameter and is formed via a double-restack powder-in-tube process that results in 18 bundles of 37 filaments. The inner sheaths are Ag, and the outermost sheath, onto which the insulation is deposited, is a Ag–Mg alloy. One length of Bi2212 wire is coated with a ~12.8 μm thick layer of doped-titania in a polyimide matrix. A second length is coated with an identical layer and subsequently with an additional ~6.6 μm thick "topcoat" of the polyimide. For comparison, a bare Bi2212 wire and a Bi2212 wire heat treated with braided-mullite insulation are also prepared.

Short samples (5-cm length) of each type of Bi2212 wire are heat treated together using a partial melt process optimized for this wire [21]–[23]. During heat treatment, the polyimide matrix burns off; hence, after heat treatment, only the ~8-μm-thick layer of doped-titania insulation remains. To attach contacts for transport measurements, the insulation is

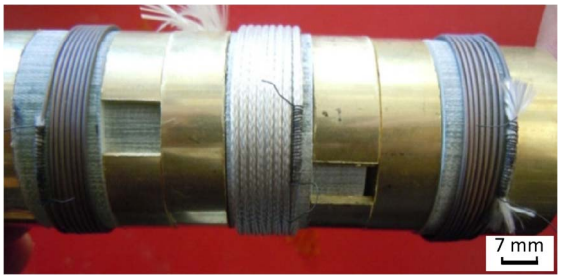

Fig. 2. Bi2212 coils after heat treatment. (From left to right) Insulated with doped titania with a polyimide topcoat, insulated with mullite, and insulated with doped titania without a polyimide topcoat. The nichrome heaters are seen as well. Note that the polyimide burns out during heat treatment.

removed from the ends of the doped-titania-insulated samples using sandpaper. Tweezers are used to gently remove the insulation around the circumference of the wire for the voltage tap attachment. For the wires heat treated within braided-mullite insulation, the mullite sheath is removed after heat treatment from the Bi2212 wires (to facilitate electrical measurements) by pulling the sheath off the wire. Sandpaper is also used to gently clean the wire surface where the mullite fibers remained fixed to the surface.

Coils: Small coils for quench studies are prepared using the same batches of insulated wire used for short-sample testing. Thus, three coils are wound, i.e., one coated with doped titania in a polyimide matrix, one coated with doped titania in a polyimide matrix and subsequently a polyimide topcoat, and one insulated with traditional braided mullite. Each is a single-layer coil, composed of eight turns, wound on an Inconel mandrel (34 mm in diameter) using $\sim$1 m of insulated wire. Each coil is wound by hand; no instrumentation is used to control the winding tension.

Each coil is instrumented with a wire heater that is used to induce a normal zone during quench studies. The heaters are made from $\sim$16-cm-long nichrome wire that is tightly wrapped around the wire covering a length of $\sim$1.5 cm. For the mullite-insulated coil, the heater is wound directly on the mullite braid. For the doped-titania insulated coils, a layer of mullite is situated between the heater and the insulation; this provides identical heating conditions to each of the wires for comparison. Each heater has an electrical resistance of $\sim$5 Ω at 4.2 K. VGE-7031 varnish is used to adhere the heater to the wire surface. The three coils are heat treated together with the short samples; Fig. 2 shows the photographs of the coils after heat treatment. Note that the polyimide burns off during heat treatment.

After heat treatment, the coils are transferred to a Garolite (G-10) coil former and instrumented with an array of voltage taps (25-μm-diameter Cu wires) for I_c measurements and quench propagation studies; the wiring configuration is illustrated in Fig. 3. Voltage taps are situated every two turns and for end-to-end (ETE) measurements. Lastly, the Bi2212 coils are vacuum impregnated with Stycast 1266 epoxy.

3) YBCO Coils: YBCO pancake coils are wound using 4-mm-wide $\sim$0.1-mm-thick CC from SuperPower, Inc. The conductor has a Hastelloy substrate and a 20-μm-thick copper stabilizer on all sides [24]. Three coils are prepared. Two coils are insulated by coating the conductor with one of the two slurries used to prepare samples for thermal conductivity measurements; thus, there is one coil with the larger doped-titania particles in a polyimide matrix and one insulated with the smaller doped-titania particles in polyimide. The insulating coatings are about 11 μm thick, and no additional insulation is used to electrically isolate the turns of the coils. Note that the YBCO conductor does not require a heat treatment; hence, the polyimide remains present. The third coil is wound with the same YBCO conductor but with a 50-μm-thick Kapton tape as the turn-to-turn insulation. All three YBCO coils are wound on a G-10 coil form with a 63.5-mm inner diameter. Each coil consists of five turns, requiring $\sim$1 m of conductor; Fig. 4 shows the photographs of the coils.

Similar to the Bi2212 coils, the YBCO coils are instrumented with a heater and an array of voltage taps; the specifics are seen in the schematic shown in Fig. 5. The heaters, which cover a length of $\sim$1.5 cm, are made from a $\sim$15-cm-long Lakeshore WNC-32 nichrome wire with a resistance of $\sim$5 Ω at 77 K. The heaters are attached to the outside surfaces of the pancake coils with Lakeshore VGE-7031 insulating varnish. A small amount of Stycast 2850 black epoxy is applied over the heater to reduce cooling. The voltage taps, made from 25-μm-thick 1.5-mm-wide Cu ribbons, are soldered to the edge of the YBCO to avoid electrical contact between neighboring conductors. A small amount of VGE-7031 varnish is used to improve the mechanical stability of the contacts. Lastly, the YBCO coils are vacuum impregnated with Stycast 1266 epoxy.

B. Thermal Conductivity

Thermal conductivity of the polyimide and polyimide/doped-titania films is measured using the 3ω method [25], which facilitates thermal conductivity measurements of thin films that would otherwise be very difficult due to their small mass [26], [27]. An electrical schematic of the 3ω measurement system is shown in Fig. 6.

A digital lock-in amplifier generates a sinusoidal signal and provides a precise frequency reference. Two differential amplifiers are used to subtract the fundamental frequency from the signal and to amplify the higher harmonics. The third harmonic, which is proportional to the thermal conductivity, is extracted using a lock-in amplifier. The in-phase component between 100 and 10 000 Hz is recorded, and the thermal conductivity is found from the slope of the resulting curve.

Thermal conductivity is measured at RT, 77 K, and 4.2 K. Samples are mounted onto stages specifically designed for the measurement temperature. The stage for RT measurements is made of gold-plated nickel and is attached onto a brass chuck surrounded by a heater coil that is connected to a power supply. A type-K chromel–alumel thermocouple is embedded in epoxy on the surface of the chuck to monitor the stage temperature. This stage is housed in a Faraday cage to shield electrical noise. Electrical connections to the four-point contact pads of the heater wire on the sample are made via probes attached onto a micropositioner.

For 77-K and 4.2-K measurements, the sample stage is made with a plate of G-10. Gold wires are soldered to the four-point

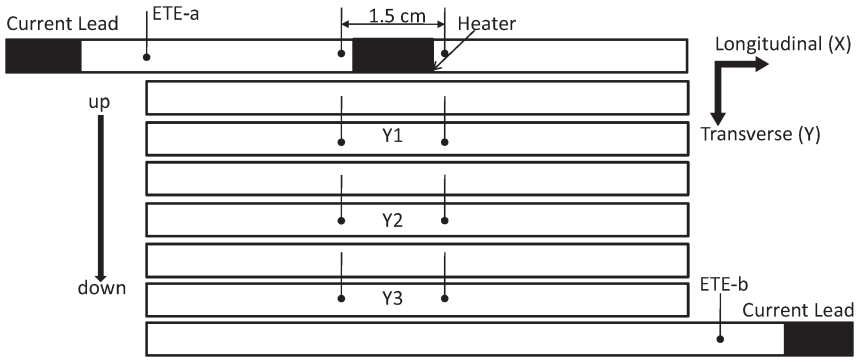

Fig. 3. Schematic of the voltage tap positions, current leads, and heater for the Bi2212 coils.

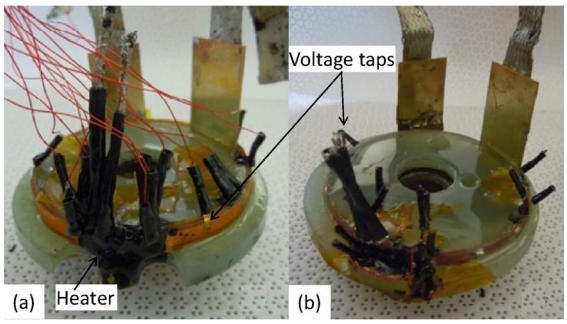

Fig. 4. Instrumented YBCO coils with (a) Kapton insulation and (b) doped-titania insulation.

contact pads on the sample, and the sample is mounted to the G-10 stage. The gold wires are then connected to copper connector block contacts that surround the edge of the stage. The copper connector blocks are used to connect to the instrumentation (current and voltage) for the measurement. Thermocouples are epoxied to the stage and to the sample to monitor the temperature. The stage is then immersed into a cryostat that is filled with either liquid nitrogen or liquid helium.

The approach is first validated using measurements of sapphire, silicon, and glass and compared the results to published values. Subsequently, the thermal conductivity of each sample is measured several times at different locations on the sample and repeated several times to reduce the measurement error.

C. Critical Current

The critical current I_c of short samples is measured at self-field in liquid helium using the standard four-probe technique. The voltage-tap spacing is 20 mm on each sample, and a 1-μV/cm electric field criterion is used to determine I_c. Two samples of each type are independently measured. After measuring I_c, the sample surfaces and cross sections are imaged in a JEOL JSM-6010LA scanning electron microscope (SEM).

The self-field I_c as a function of location is measured on the Bi2212 coils at 4.2 K. Similar to the short-sample measurements, I_c is determined for each section using a 1-μV/cm electric field criterion.

D. Quench Measurements

Quench experiments follow similar protocols as previously reported quench experiments [10], [15], [16], [18]. Bi2212 coils are quenched at 4.2 K, self-field. After initiating a 100-A transport current in the coil, quenches are induced by a 0.3-s 50-V pulse into the heater wire, corresponding to 20 J of energy. Voltage versus time is monitored and recorded for all voltage taps. After completing the testing of Bi2212 coils, the mullite-insulated coil is deconstructed into short samples and the transport I_c is measured at 4.2 K in self-field.

The quench behavior of the three YBCO coils is measured at 77 K, self-field, and subsequently at 4.2 K and 5 T. For 77-K measurements, the coils are operating with a 60-A transport current, whereas for the 4.2-K 5-T measurements, separate quench measurements are made with transport currents of 150 and 250 A. All YBCO coil quenches are induced by a 0.3-s 50-V heater pulse, corresponding to 20 J of heat. For the 4.2-K measurements, the magnetic field is oriented parallel to the wide face of the tape (i.e., the superconducting magnet providing the background magnetic field and the YBCO pancake coils are coaxial). The quench test protocols for the YBCO coils are otherwise the same as for the Bi2212 coils.

NZPVs are calculated directly from the voltage–time data. The NZPV is equal to the distance between neighboring voltage taps divided by the time delay between each of the taps reaching a voltage criterion chosen such that the voltage–time curves are nearly parallel (see, for example, [8, Fig. 11]). For the Bi2212 coils, the voltage criterion is 0.010 V, whereas for the YBCO coils, a 0.050-V criterion is used.

III. Results and Discussion

A. Thermal Conductivity

Thermal conductivity measurement results for sapphire (36 W/m·K), silicon (147 W/m·K), and glass (1.1 W/m·K) are within 4% of published values for these materials, confirming the measurement approach. The thermal conductivity values of the polyimide and the doped-titania (small and large particle) insulation coatings at RT, 77 K, and 4.2 K are shown in Table II. The nanoparticle additions significantly increase the thermal conductivity at all temperatures; ~4 times higher at RT and 77 K and about an order of magnitude at 4.2 K. In addition, included in the table are values for Kapton [28], [29]; note that the thermal conductivity of the doped-titania insulation is a factor of 5 greater than Kapton at RT, a factor of 3 at 77 K, and a factor of 10 at 4.2 K. For mullite, the RT values vary

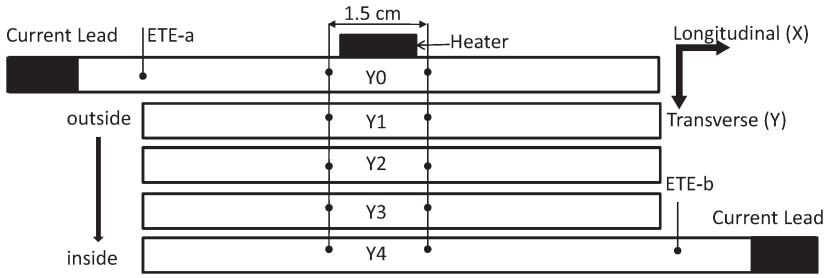

Fig. 5. Schematic of the voltage tap positions, current leads, and heater for the YBCO coils.

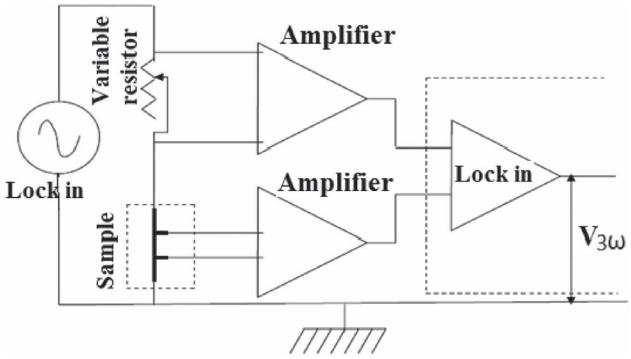

Fig. 6. Schematic of the electronics used for the 3ω thermal conductivity measurements. The amplifiers are analog design models AD620 for the RT and 77-K measurements and models AD624 for the 4.2-K measurements. The lock-in amplifiers are Stanford Research model 830.

greatly in the literature, and low temperature data have not been published.

B. Critical Current of Bi2212 Short Samples and Coils

The average I_c values of the Bi2212 short samples measured at 4.2 K are 629 A for bare wires, 582 A for wires with doped-titania insulation, 580 A for wires with doped-titania and a polymer topcoat, and 608 A for wires with braided-mullite insulation. These values showed less than 10% variance for each sample type. These results confirm that the heat treatment is effective and that the insulation does not have significant deleterious reactions with the Bi2212 wires.

Fig. 7 shows cross-sectional SEM micrographs of Bi2212 short samples after heat treatment. The edge of the doped-titania insulated wire with a polymer topcoat is smoother than that of the doped-titania insulated wire without the topcoat. The edge of the wire with braided-mullite insulation is coarse, indicating a reaction between the mullite and wire.

Fig. 8 shows 4.2 K, self-field I_c as a function of location within the Bi2212 coils (and ETE values as well); the short-sample data are shown for comparison. The transport I_c of the doped-titania insulated coils is homogeneous and about 70% of short sample. The ETE I_c of the mullite-insulated coil is only 170 A due to the low I_c in turns 1 and 2 (139 A). Thus, it is not possible to measure I_c in turns 3–8 as the coil voltage limit is reached with a transport current of 290 A; hence, all that can be said of turns 3–8 is that $I_c > 290$ A. After all measurements of the coil are complete, including quench experiments, the mullite-insulated coil is deconstructed into short samples and the transport I_c is measured at 4.2 K, self-field. The average I_c of samples from turns 3 to 8 is 392 A and is also plotted in Fig. 8.

Some of the difference between short sample and coil I_cs is due to the increased self-field in the coils. Previous work indicates that the critical current density in Bi2212 wires and coils tends to decrease as the length of wire increases due to the agglomeration of porosity during heat treatment [30]; this also likely contributes to the difference between short-sample and coil I_c. There is also evidence that interactions with mullite can reduce critical current; it is unclear if the low I_c in turns 1 and 2 is due to such interactions or if the conductor was damaged during winding [31].

C. Quench Behavior

1) Bi2212 Coils: Fig. 9 shows the voltage versus time in the transverse direction within the Bi2212 coils during a quench. The transverse NZPVs, determined directly from the voltage–time data, are quantified in Table III. The results show that the doped-titania insulation increases the transverse NZPV by a factor of 2.7 relative to the mullite-insulated coil. Note that propagation in the mullite-insulated coil is not sufficient that a propagation velocity for Y2 $\rightarrow$ Y3 can be determined. The coil with the polyimide topcoat, which burns out during heat treatment, shows about a 5% slower propagation velocity than the coil without the topcoat. It is not clear if this is related to the topcoat or simply an experimental variation.

2) YBCO Coils: Fig. 10 shows voltage versus time data in the transverse direction for the YBCO coils during a quench at 77 K, self-field, and a transport current of 60 A. Figs. 11 and 12 show data from the same coils at 4.2 K and 5 T with transport currents of 150 and 250 A, respectively. Tables IV and V summarize the normal zone propagation results.

For the YBCO coils tested at 77 K, self-field, the doped-titania insulation increases the transverse NZPV by a factor of 2.8 relative to the Kapton-insulated coil. At 4.2 K, 5 T, and 150 A, the NZPV is increased by a factor of 2.1, and when the transport current is increased to 250 A, the NZPV in the doped-titania coil is 2.5 times greater than that in the Kapton-insulated coil.

3) Discussion: The graphs in Figs. 9–12 indicate that there is a time delay before the onset of a quench. Note that, in all experiments, the heat pulse that creates the normal zone begins at $t = 0.3$ s. The voltages graphed in Figs. 9–12 are not on the turn with the heater, as illustrated in the schematics in Figs. 3 and 5. Thus, the delay represents the propagation time from the heater to the nearest turn with voltage taps. The turn with

TABLE II
THERMAL CONDUCTIVITY VALUES K_s OF POLYIMIDE AND DOPED-TITANIA INSULATION COATINGS AS A FUNCTION OF TEMPERATURE (MEASURED HERE); LITERATURE VALUES FOR KAPTON ARE INCLUDED AS WELL

Sample type	K_s (W/m·K), 300 K	K_s (W/m·K), 77 K	K_s (W/m·K), 4.2 K
Polyimide	0.26 +/-0.03	0.10 +/-0.02	0.008 +/-0.005
Doped-titania insulation (small nanoparticles)	1.05 +/-0.1	0.38 +/-0.05	0.09 +/-0.03
Doped-titania insulation (large nanoparticles)	0.95 +/-0.1	0.40 +/-0.05	0.10 +/-0.03
Kapton [28, 29]	0.19	0.13	0.010

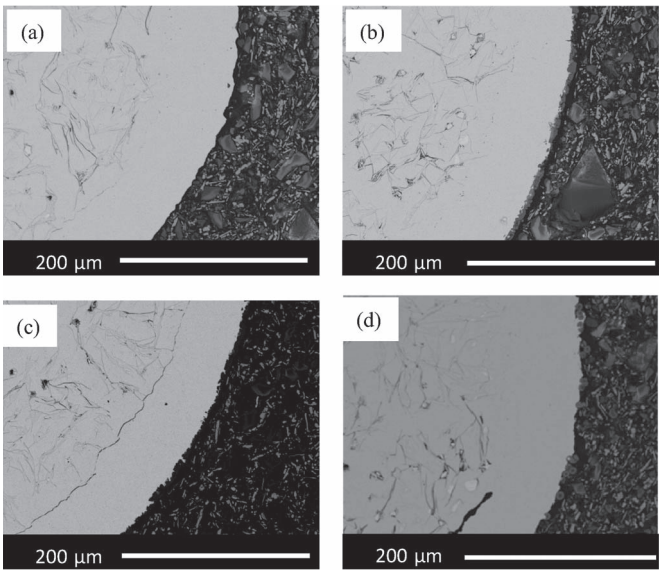

Fig. 7. Cross-sectional images of the outer edges of Bi2212 wires after heat treatment: (a) bare wire; (b) doped-titania insulated wire; (c) doped-titania insulated wire with a polyimide topcoat; and (d) wire with braided-mullite insulation. Note that the polyimide burns out during heat treatment.

the heater is not used for calculating the NZPV because the behavior is overly influenced by the heat pulse rather than the more intrinsic propagation.

The effects of the doped-titania insulation on the NZPV, relative to conventional insulation coatings, are remarkably consistent, with propagation increasing by factors ranging from 2.1 to 2.8. It is interesting to compare the results for the YBCO coils with increasing transport current; the NZPV for the doped-titania insulated coil nearly doubled when the current was increased from 150 to 250 A, whereas the increase in propagation velocity in the Kapton-insulated coil was only about 50%. During a quench, increased transport current corresponds to increased joule heating in the normal zone. Thus, at higher transport current and higher joule heating, the effectiveness of increased turn-to-turn thermal conductivity is also increased. The small size of the Bi2212 and YBCO coils may minimize the effects of the insulation due to the effects of cooling at the coil surface. In large epoxy-impregnated coils, the increase in NZPV relative to Kapton or mullite is likely to be significantly greater.

It is important to note that, because the doped-titania insulation is significantly thinner than the mullite braid and the Kapton, the overall current density of a magnet is significantly increased. This increases the magnetic field generated per ampere of current (the "coil constant"), reducing conductor costs for large magnets. Reduced insulation thickness also results in reduced specific heat (due to the reduction in the volume of material), which also accelerates normal zone propagation. Considering the coils studied here, the volume of the doped-titania insulated Bi2212 coil is 37% less than that of the mullite-insulated coil and the volume of the doped-titania YBCO coils is 25% less than that of the Kapton-insulated coil. Because these coils have a relatively small diameter, it is difficult to determine precisely how much the increase in NZPV found here is due to the increased thermal conductivity and how much is due to the decrease in specific heat without detailed modeling; the impact on coil performance, however, is evident.

It is also interesting to compare the results from the Bi2212 coil to those from the YBCO coil. While the NZPV varies with operating current and temperature, the NZPVs in the YBCO coils at 4.2 K are significantly faster than those in the Bi2212 coils. This is primarily due to the coil geometries. The Bi2212 coils are RWs; hence, the turn-to-turn contact is that of two adjacent circles. If the wires are perfectly round and the coil is perfectly wound, then there is only point-to-point contact between the insulated wires. The epoxy fills in the gaps; thus, a more thermally conducting epoxy would further enhance propagation. The YBCO coils, however, are pancake wound; thus, the turn-to-turn contact area is that of the wide face of the conductor and the effects of increased turn-to-turn thermal conductivity are most pronounced.

IV. SUMMARY

A thin thermally conducting electrical insulation based upon doped-titania nanoparticles has been studied for the turn-to-turn insulation in Bi2212 and YBCO coils. The doped-titania nanopowders are incorporated into a polyimide matrix and applied to the surface of the superconducting wires. The insulation is also deposited on standard substrates in order to measure its thermal conductivity as a function of temperature. The chemical compatibility of the insulation with Bi2212 wires is studied through measurements of the transport critical current of Bi2212 wires and coils, as compared with bare wires and mullite-insulated wires. The impact on the NZPV of Bi2212 and YBCO coils is measured and compared with the NZPV of coils insulated with mullite and Kapton.

Results show that the doped titania significantly increases the thermal conductivity of polyimide, particularly at 4.2 K. As a

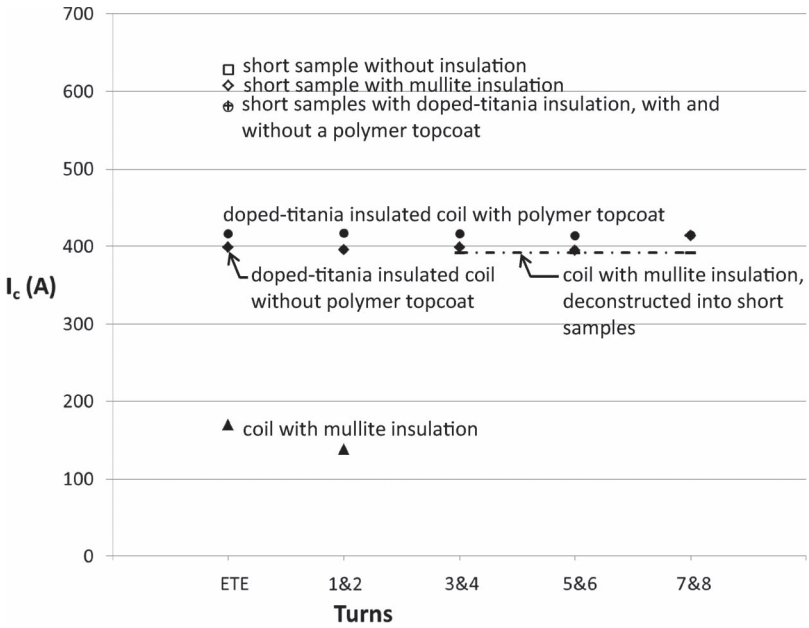

Fig. 8. I_c of 4.2 K, self-field, as a function of location within the Bi2212 coils (and ETE values as well); the short-sample data are also shown for comparison. Note that in the mullite coil, because of the low I_c in sections 1 and 2, it was not possible to ramp the current sufficiently high to determine the critical current in sections 3–8. Thus, I_c values for those sections are obtained by deconstructing the coil and measuring short samples after quench testing is completed.

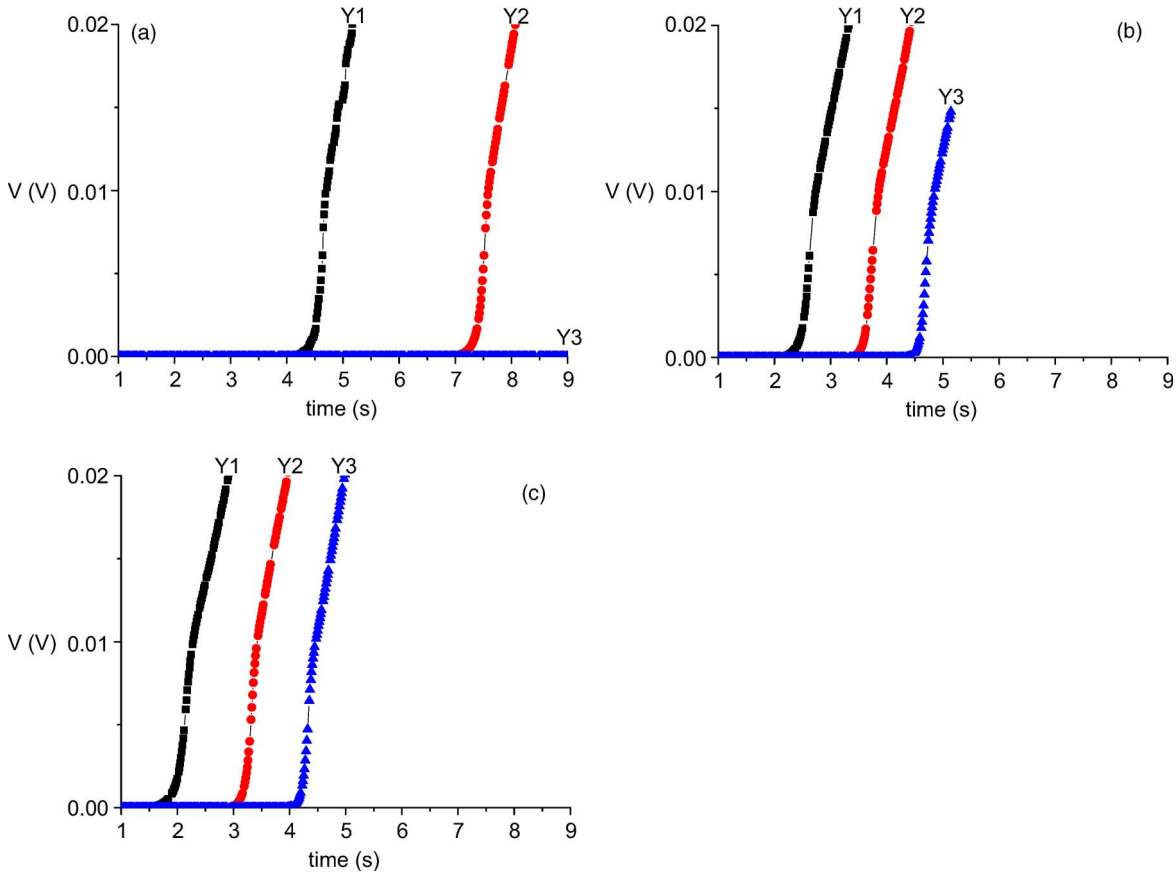

Fig. 9. Voltage versus time and location in the Bi2212 coils during quenching at 4.2 K, self-field. See Fig. 4 for the definitions of Y1, Y2, and Y3 (voltage tap locations within the coils). (a) Bi2212 coil with braided-mullite insulation. (b) Bi2212 coil with doped-titania insulation. (c) Bi2212 coil with doped-titania insulation and a polyimide topcoat.

result, the doped-titania-based insulation has a thermal conductivity value that is an order of magnitude greater than that of Kapton in liquid helium. Short-sample and coil measurements of doped-titania insulated Bi2212 show no deleterious reactions between the insulation and the Bi2212 wire. No significant reduction in the critical current density of the Bi2212 wires is

TABLE III
TRANSVERSE (TURN-TO-TURN) NORMAL ZONE PROPAGATION VELOCITIES AT 4.2 K, SELF-FIELD, FOR BI2212 COILS WITH MULLITE AND DOPED-TITANIA INSULATION (TRANSPORT CURRENT = 100 A)

Sections	Braided mullite insulated Bi2212 coil	Doped-titania insulated Bi2212 coil	Doped-titania insulated Bi2212 coil with a polymer topcoat
Y1→Y2	0.69 layer/s (1.459 s/layer)	1.79 layer/s (0.559 s/layer)	1.74 layer/s (0.576 s/layer)
Y2→Y3	--	1.99 layer/s (0.502 s/layer)	1.93 layer/s (0.518 s/layer)
Average	0.69 layer/s (1.459 s/layer)	1.89 layer/s (0.531 s/layer)	1.84 layer/s (0.547 s/layer)

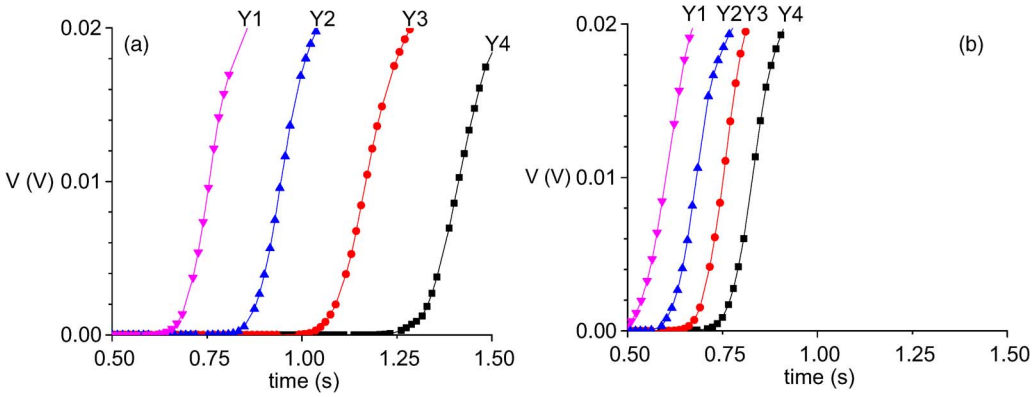

Fig. 10. Voltage versus time and location in the YBCO pancakes during quenching at 77 K, self-field, with a transport current of 60 A. See Fig. 6 for the definitions of Y1, Y2, Y3, and Y4 (voltage tap locations within the coils). (a) Kapton-insulated coil. (b) Doped-titania insulated coil.

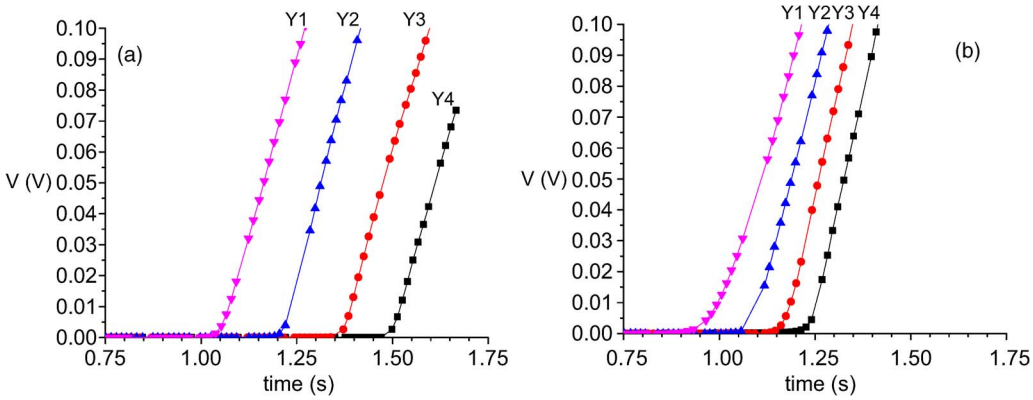

Fig. 11. Voltage versus time and location in the YBCO pancakes during quenching at 4.2 K and 5 T with a transport current of 150 A. See Fig. 6 for the definitions of Y1, Y2, Y3, and Y4 (voltage tap locations within the coils). (a) Kapton-insulated coil. (b) Doped-titania insulated coil.

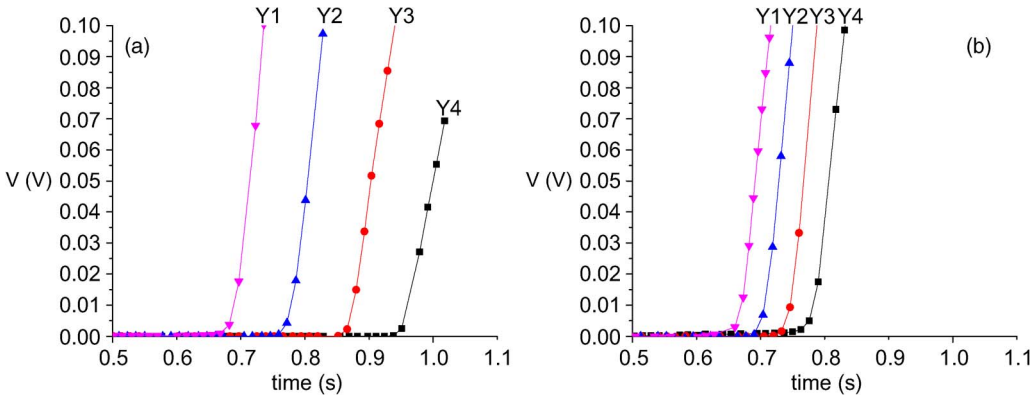

Fig. 12. Voltage versus time and location in the YBCO pancakes during quenching at 4.2 K and 5 T with a transport current of 250 A. See Fig. 6 for the definitions of Y1, Y2, Y3, and Y4 (voltage tap locations within the coils). (a) Kapton-insulated coil. (b) Doped-titania insulated coil.

TABLE IV
TRANSVERSE (TURN-TO-TURN) NORMAL ZONE PROPAGATION VELOCITIES AT 77 K, SELF-FIELD, FOR YBCO PANCAKE COILS WITH KAPTON AND DOPED-TITANIA INSULATION COATINGS (TRANSPORT CURRENT = 60 A)

Sections	Kapton insulated	Doped-titania insulated (large nanoparticles)	Doped-titania insulated (small nanoparticles)
Y1→Y2	5.15 layers/s (0.194 s/layer)	12.82 layers/s (0.078 s/layer)	15.63 layers/s (0.064 s/layer)
Y2→Y3	4.50 layers/s (0.222 s/layer)	13.70 layers/s (0.073 s/layer)	12.34 layers/s (0.081 s/layer)
Y3→Y4	4.12 layers/s (0.243 s/layer)	12.66 layers/s (0.079 s/layer)	13.33 layers/s (0.075 s/layer)
Average	4.59 layers/s (0.219 s/layers)	13.06 layers/s (0.077 s/layers)	13.76 layers/s (0.073 s/layers)

TABLE V
TRANSVERSE (TURN-TO-TURN) NORMAL ZONE PROPAGATION VELOCITIES AT 4.2 K AND 5 T FOR YBCO PANCAKE COILS WITH KAPTON AND DOPED-TITANIA INSULATION COATINGS

Sections	I_t = 150 A		I_t = 250 A	
	Kapton insulated	Doped-titania insulated	Kapton insulated	Doped-titania insulated
Y1→Y2	6.71 layer/s (0.149 s/layer)	13.70 layer/s (0.073 s/layer)	11.11 layer/s (0.09 s/layer)	27.03 layer/s (0.037 s/layer)
Y2→Y3	6.02 layer/s (0.166 s/layer)	14.29 layer/s (0.070 s/layer)	10.10 layer/s (0.099 s/layer)	26.32 layer/s (0.038 s/layer)
Y3→Y4	7.52 layer/s (0.133 s/layer)	14.49 layer/s (0.069 s/layer)	10.31 layer/s (0.097 s/layer)	25.00 layer/s (0.040 s/layer)
Average	6.75 layer/s (0.149 s/layer)	14.16 layer/s (0.071 s/layer)	10.51 layer/s (0.095 s/layer)	26.11 layer/s (0.038 s/layer)

found. Furthermore, the insulation survives the heat treatment intact. Relative to mullite-insulated Bi2212 coils and Kapton-insulated YBCO coils, the turn-to-turn normal zone propagation velocities of doped-titania insulated coils are increased by factors ranging from 2.1 to 2.8 in measurements at 77 K in liquid nitrogen and at 4.2 K in liquid helium (self-field and at 5 T).

These results indicate that doped-titania insulation has the potential to significantly improve the performance of HTS-based superconducting magnets. Increased NZPV, without a reduction in MQE, simplifies quench detection and quench protection. A thinner insulation system results in high coil current density, increasing the magnetic field generated per ampere of current and significantly reducing conductor costs for large magnets.

ACKNOWLEDGMENT

The authors would also like to thank Y. Zhang for the scanning electron microscope images.

REFERENCES

[1] J. Schwartz, T. Effio, X. Liu, Q. V. Le, A. L. Mbaruku, H. J. Schneider-Muntau, T. Shen, H. Song, U. P. Trociewitz, X. R. Wang, and H. W. Weijers, "High field superconducting solenoids via high temperature superconductors," *IEEE Trans. Appl. Supercond.*, vol. 18, no. 2, pp. 70–81, Jun. 2008.

[2] R. Gupta, M. Anerella, J. Cozzolino, J. Escallier, G. Ganetis, A. Ghosh, M. Harrison, A. Marone, J. Muratore, J. Schmalzle, W. Sampson, and P. Wanderer, "Status of high temperature superconductor magnet R&D at BNL," *IEEE Trans. Appl. Supercond.*, vol. 14, no. 2, pp. 1198–1201, Jun. 2004.

[3] S. Gao, K. T. Chau, C. H. Liu, D. Y. Wu, and J. G. Li, "SMES control for power grid integrating renewable generation and electric vehicles," *IEEE Trans. Appl. Supercond.*, vol. 22, no. 3, p. 5 701 804, Jun. 2012.

[4] B. K. Kang, S. T. Kim, B. C. Sung, and J. W. Park, "A study on optimal sizing of superconducting magnetic energy storage in distribution power system," *IEEE Trans. Appl. Supercond.*, vol. 22, no. 3, p. 5 701 004, Jun. 2012.

[5] D. U. Gubser, "Superconductivity: An emerging power-dense energy-efficient technology," *IEEE Trans. Appl. Supercond.*, vol. 14, no. 4, pp. 2037–2046, Dec. 2004.

[6] G. Snitchler, B. Gamble, and S. S. Kalsi, "The performance of a 5 MW high temperature superconductor ship propulsion motor," *IEEE Trans. Appl. Supercond.*, vol. 15, no. 2, pp. 2206–2209, Jun. 2005.

[7] D. W. Hazelton, M. T. Gardner, J. A. Rice, M. S. Walker, C. M. Trautwein, P. Haldar, D. U. Gubser, M. Superczynski, and D. Waltman, "HTS coils for the Navy's superconducting homopolar motor/generator," *IEEE Trans. Appl. Supercond.*, vol. 7, no. 2, pp. 664–667, Jun. 1997.

[8] X. Wang, U. P. Trociewitz, and J. Schwartz, "Near-adiabatic quench experiments on short $YBa_2Cu_3O_{7-\delta}$ coated conductors," *J. Appl. Phys.*, vol. 101, no. 5, p. 053904, Mar. 2007.

[9] X. Wang, U. P. Trociewitz, and J. Schwartz, "Critical current degradation of short $Yba_2Cu_3O_{7-s}$ coated conductor due to an unprotected quench," *Supercond. Sci. Technol.*, vol. 24, no. 3, p. 035006, Mar. 2011.

[10] X. R. Wang, A. R. Caruso, M. Breschi, G. M. Zhang, U. P. Trociewitz, H. W. Weijers, and J. Schwartz, "Normal zone initiation and propagation in Y–Ba–Cu–O coated conductors with Cu stabilizer," *IEEE Trans. Appl. Supercond.*, vol. 15, no. 2, pp. 2586–2589, Jun. 2005.

[11] X. R. Wang, U. P. Trociewitz, and J. Schwartz, "Self-field quench behavior of YBCO coated conductors with different stabilizers," *Supercond. Sci. Technol.*, vol. 22, no. 8, p. 085005, Aug. 2009.

[12] H. Song, K. Gagnon, and J. Schwartz, "Quench behavior of conduction-cooled $YBa_2Cu_3O_{7-\delta}$ coated-conductor pancake coils stabilized with brass and copper," *Supercond. Sci. Technol.*, vol. 23, no. 10, p. 109 802, Oct. 2010.

[13] H. H. Song and J. Schwartz, "Stability and quench behavior of $YBa_2Cu_3O_{7-x}$ coated conductor at 4.2 K, self-field," *IEEE Trans. Appl. Supercond.*, vol. 19, no. 5, pp. 3735–3743, Oct. 2009.

[14] C. L. H. Thieme, K. Gagnon, H. Song, and J. Schwartz, "Stability of second generation HTS pancake coils at 4.2 K for high heat flux

applications," *IEEE Trans. Appl. Supercond.*, vol. 19, no. 3, pp. 1626–1632, Jun. 2009.
[15] F. Trillaud, A. Caruso, J. Barrow, B. Trociewitz, U. P. Trociewitz, H. W. Weijers, and J. Schwartz, "Normal zone generation and propagation in $YBa_2Cu_3O_{7-\delta}$ coated conductors initialized by localized pulsed disturbances," in *Proc. Adv. Cryog. Eng. Mater.*, 2003, pp. 852–859.
[16] F. Trillaud, H. Palanki, U. P. Trociewitz, S. H. Thompson, H. W. Weijers, and J. Schwartz, "Normal zone propagation experiments on HTS composite conductors," *Cryogenics*, vol. 43, no. 3–5, pp. 271–279, Mar.–May 2003.
[17] T. Effio, U. P. Trociewitz, X. Wang, and J. Schwartz, "Quench induced degradation in $Bi_2Sr_2CaCu_2O_{8+x}$ tape conductors at 4.2 K," *Supercond. Sci. Technol.*, vol. 21, no. 4, p. 045010, Apr. 2008.
[18] U. P. Trociewitz, B. Czabaj, S. Hong, Y. Huang, D. C. Knoll, D. C. Larbalestier, W. D. Markiewicz, H. Miao, M. Meinesz, X. Wang, and J. Schwartz, "Quench studies on a layer-wound $Bi_2Sr_2CaCu_2Ox$/AgX coil at 4.2 K," *Supercond. Sci. Technol.*, vol. 21, no. 2, p. 025015, Feb. 2008.
[19] M. Phillips, "Influence of turn-to-turn insulation on quench propagation in YBCO coated conductors," M.S. thesis, Dept. Mech. Eng., Florida A&M Univ., Tallahassee, FL, USA, 2009.
[20] D. M. MacLeod, "Wire-wound rod coating," in *Coatings Technology Handbook*, 3rd ed. Boca Raton, FL, USA: CRC, 2005.
[21] K. R. Marken, H. P. Miao, M. Meinesz, B. Czabaj, and S. Hong, "Progress in Bi-2212 wires for high magnetic field applications," *IEEE Trans. Appl. Supercond.*, vol. 16, no. 2, pp. 992–995, Jun. 2006.
[22] H. Miao, K. R. Marken, M. Meinesz, B. Czabaj, and S. Hong, "Development of round multifilament Bi-2212/Ag wires for high field magnet applications," *IEEE Trans. Appl. Supercond.*, vol. 15, no. 2, pp. 2554–2557, Jun. 2005.
[23] T. Shen, J. Jiang, F. Kametani, U. P. Trociewitz, D. C. Larbalestier, J. Schwartz, and E. E. Hellstrom, "Filament to filament bridging and its influence on developing high critical current density in multifilamentary $Bi_2Sr_2CaCu_2O_x$ round wires," *Supercond. Sci. Technol.*, vol. 23, no. 2, p. 025009, Feb. 2010.
[24] D. W. Hazelton, V. Selvamanickam, J. M. Duval, D. C. Larbalestier, W. D. Markiewicz, H. W. Weijers, and R. L. Holtz, "Recent developments in 2G HTS coil technology," *IEEE Trans. Appl. Supercond.*, vol. 19, no. 3, pp. 2218–2222, Jun. 2009.
[25] D. G. Cahill and R. O. Pohl, "Thermal-conductivity of amorphous solids above the plateau," *Phys. Rev. B*, vol. 35, no. 8, pp. 4067–4073, Mar. 15, 1987.
[26] C. Mion, "Investigation of the thermal properties of gallium nitride using the three omega technique," Ph.D. dissertation, Dept. Electron. Eng., North Carolina State Univ., Raleigh, NC, USA, 2005.
[27] D. G. Cahill, "Thermal conductivity measurement from 30 to 750 K: The 3 omega method," *Rev. Sci. Instrum.*, vol. 61, no. 2, pp. 802–808, Feb. 1990.
[28] *Cryogenic Materials Properties Program SC, Release B-01*, CI Center, Boulder, CO, USA, 2001.
[29] J. Lawrence, A. B. Patel, and J. G. Brisson, "The thermal conductivity of Kapton HN between 0.5 and 5 K," *Cryogenics*, vol. 40, no. 3, pp. 203–207, Mar. 2000.
[30] A. Malagoli, F. Kametani, J. Jiang, U. P. Trociewitz, E. E. Hellstrom, and D. C. Larbalestier, "Evidence for long range movement of Bi-2212 within the filament bundle on melting and its significant effect on J_c," *Supercond. Sci. Technol.*, vol. 24, no. 7, p. 075016, Jul. 2011.
[31] X. T. Liu, W. T. Nachtrab, T. Wong, and J. Schwartz, "Effect of resolidification conditions on $Bi_2Sr_2CaCu_2O_x$/Ag/AgMg coil performance," *IEEE Trans. Appl. Supercond.*, vol. 19, no. 3, pp. 2232–2236, Jun. 2009.

Sasha Ishmael (S'07–M'08) received the Ph.D. degree in electrical engineering from Florida Institute of Technology, Melbourne, FL, USA, in 2010.

During her Ph.D. studies, she was a Visiting Scholar at the Nancy Electronic and Electro-technical Research Group (GREEN) Laboratory, Université Henri Poincaré, Nancy, France, where she carried out work on magnetic switching of MgB_2. She is currently a Postdoctoral Research Scholar in the Department of Materials Science and Engineering, North Carolina State University, Raleigh, NC, USA. Prior to her present position, she was an Engineer at the Advanced Magnet Lab Inc., where she worked on the design and test of superconducting and resistive magnets for a variety of applications, including high-energy physics research, medical, and power systems. Her current research interests are focused on the testing of materials and sensors for integration with superconducting magnets to improve stability and performance.

Haojun Luo received the B.S. degree in materials science from Nanjing University, Nanjing, China, in 2003, the M.S. degree in physics from Peking University, Beijing, China, in 2006, and the Ph.D. degree from North Carolina State University, Raleigh, NC, USA, in 2013.

He developed a 3ω thermal conductivity measurement system. This system is capable of measuring thermal conductivity from 4.2 to 450 K. He uses this measurement system to investigate a variety of bulk and thin-film materials. In this paper, he measured the thermal conductivity values of nanoparticle-doped polyimide thin films at 4.2, 77, and 300 K. He also works on developing high-performance amorphous metal-oxide-semiconductor-based thin-film transistors and circuits.

Marvis White received the B.Sc. degree from The University of Tennessee, Knoxville, TN, USA, in 1973, and the M.Sc. degree from Tennessee Technological University, Cookeville, TN, in 1976, both in engineering science with a specialty in materials science.

He is currently a Senior Research Scientist at nGimat, Lexington, KY, USA, where joined in 1999 as a Project Manager for development and application of oxide template layers for the growth of YBCO superconductor films. He is currently focused on the development of electrical insulation coatings, both for low- and high-temperature superconductors and for copper magnet wire in advanced applications such as electric vehicle motors. He was the Principal Investigator (PI) of the Department of Energy (DOE) Small Business Technology Transfer Phase I, now in Phase II, titled "Thin Robust Electrical Insulator for High Field HTS Magnets" for developing insulation coatings for YBCO and Bi2212 and the PI of the DOE Small Business Innovation Research Phase II titled "Thin, Ceramic-based Insulation for Nb_3Sn." He has been intensively involved in many areas of coating technology development within the company, including coatings for superhydrophobicity and self-cleaning, antifouling, anticorrosion, and embedded capacitors; power supercapacitors; plasmon resonance optical filtering; optical waveguides; ferroelectrics for RF devices; and so on. He also worked for two to three years on the photolithographic fabrication of photonic sensors, electrooptic modulators, and RF tunable filters and phase shifters. Prior to joining nGimat, he was a Research Engineer and a Senior Research Engineer at The University of Tennessee Space Institute, Tullahoma, TN, where he worked in superconductivity on improving the recrystallization cube texture of Ni substrate tapes and conducting XRD texture analysis of high-temperature-semiconductor thick films, oxide buffer layers, and substrates. Before that, he managed a project conducting all aspects of boiler and superheater fireside corrosion and fireside ash fouling research and testing at a DOE coal-fired MHD demonstration scale research facility over a 14-year period.

Frank Hunte received the B.Sc. and M.Sc. degrees in physics from Florida Agricultural and Mechanical University, Tallahassee, FL, USA, in 1995 and 1997, respectively, and the Ph.D. degree in physics from the University of Minnesota, Minneapolis, MN, USA, in 2004.

He is currently an Assistant Professor in the Department of Materials Science and Engineering, North Carolina State University (NCSU), Raleigh, NC, USA. Prior to joining the faculty at NCSU, he was a Visiting Assistant Scholar/Scientist at the Applied Superconductivity Center within the Magnets and Materials Division of the National High Magnetic Field Laboratory at Florida State University, Tallahassee. His current research interests include magnetic materials, high-temperature superconductors, material processing methods, and functionality and operating environments (thermal, mechanical, and electromagnetic) from basic materials physics to technological applications.

Dr. Hunte is currently a member of the National Research Council's Committee to Assess the Current Status and Future Direction of High Magnetic Field Science in the USA. The committee is tasked with assessing the needs of the U.S. research community for high magnetic fields and will provide guidance for the future of high magnetic field research and technology in the USA over the next decade.

X. T. Liu, biography not available at the time of publication.

Natalia Mandzy received the B.Sc. degree in chemical engineering from Lviv Polytechnic Institute, Lviv, Ukraine, in 1996, and the M.Sc. degree in materials science and engineering from the University of Kentucky, Lexington, KY, USA, in 2003.

She is currently a Coating Engineer at nGimat, Lexington. She develops nanoparticle/polymer composite insulating coatings for superconducting wire and tape and for electric motor application. She has an extensive experience with the development and characterization of nanocomposites, nanoparticle dispersions, and slurries. Before joining nGimat in 2011, she was a Research Engineer at the University of Kentucky in 2005–2011 and a Research and Development Engineer at Optical Dynamics Corporation in 2004–2006. She developed a surface modification technique used commercially in polymer nanocomposites, established practices to manufacture nanoparticles of consistent quality [materials prepared by these methods are used for Environmental Protection Agency (EPA) STAR Award], and evaluated nanopowders and commercial products containing nanoparticles for U.S. EPA studies.

John F. Muth (M'07) received the B.Sc. degree in applied engineering physics from Cornell University, Ithaca, NY, USA, in 1988. After serving as a Submarine Officer in the U.S. Navy, he received the Ph.D. degree in solid-state physics from North Carolina State University, Raleigh, NC, USA, in 1998.

He is currently a Professor of electrical and computer engineering at North Carolina State University. He has more than 100 peer-reviewed publications and 8 awarded patents. His research interests are the growth and fabrication of novel photonic materials and devices, as well as underwater optical communications.

Prof. Muth was a recipient of several awards, including the Office of Naval Research Young Investigator Award (2003), the National Academy of Engineers Frontiers of Science Award (2004), and a Bronze Star for meritorious service while on active duty in Iraq (2008).

Golsa Naderi was born in Arak, Iran, in 1981. She received the B.Sc. degree in material science (ceramics) and engineering from Iran University of Science and Technology, Tehran, Iran, in 2004 and the M.Sc. degree in material science and engineering from Khaje Nasir Toosi University of Technology, Tehran, in 2007. Since 2010, she has been working toward the Ph.D. degree in the Department of Materials Science and Engineering, North Carolina State University (NCSU), Raleigh, NC, USA.

From 2004 to 2009, she was a Technical Expert and Inspector in Cany Mes, Mines and Industries Engineering and Technical Services Co., Tehran, where she was working in the field of ceramic refractories for the copper industry. During her study at NCSU, she has been a Graduate Research and a Teacher Assistant. Her current research project is "Understanding processing—microstructure—properties relationships in $Bi_2Sr_2CaCu_2O_x$/Ag round wires and enhanced transport through saw-tooth processing."

Liyang Ye (S'12) received the B.S. degree in automation from Tsinghua University, Beijing, China, in 2006 and the M.S. degree from the Chinese Academy of Sciences, Beijing, China, in 2009. He is currently working toward the Ph.D. degree in the Department of Materials Science and Engineering, North Carolina State University, Raleigh, NC, USA.

His research interests include stability and quench of high-temperature superconductor with electromagnetic characterization and cryogenic instrumentation, focusing on the in-field stability and normal zone propagation and quench-induced degradation in $Bi_2Sr_2CaCu_2O_{8+x}$ round wire and MgB_2 tapes.

Andrew T. Hunt received the B.Sc. degree in geology from Auburn University, Auburn, AL, USA, in 1981; the M.Sc. degree in geology from Colorado School of Mines, Golden, CO, USA, in 1986; and the Ph.D. degree in materials science and engineering from Georgia Institute of Technology (Georgia Tech), Atlanta, GA, USA, in 1993.

He is currently the Chief Executive Officer and the Chief Technology Officer of nGimat, Lexington, KY, USA, where he has developed commercial relationships with industry-leading companies and research partnerships with key government agencies in nGimat's target markets, starting the company as a "one man operation." He has authored four book chapters, published more than 50 scientific papers, and has more than 50 patents proposed, pending, or mostly issued.

Dr. Hunt was a recipient of the SAIC Award for Best Ph.D. Paper at Georgia Tech, based on his doctoral thesis on combustion chemical vapor deposition. He was selected in 2002 for the National Academy of Engineering's Frontiers of Engineering Symposium and the 2005 German–US joint meeting. He has served on a board at the National Academies and on Georgia Tech's External Advisory Board for the School of Materials Science and Engineering (Chairman), College of Engineering, and as Trustee of the Alumni Association.

Justin Schwartz (M'91–SM'01–F'04) received the B.S. degree in nuclear engineering degree from the University of Illinois at Urbana-Champaign, Urbana, IL, USA, in 1985 and the Ph.D. degree in nuclear engineering degree from Massachusetts Institute of Technology, Cambridge, MA, USA, in 1990.

After serving as a Visiting Scientist at the National Research Institute for Metals, Tsukuba, Japan, working with Dr. H. Maeda shortly after the discovery of superconductivity in the Bi–Sr–Ca–Cu–O system, he became an Assistant Professor at the University of Illinois at Urbana-Champaign. In 1993, he joined the National High Magnetic Field Laboratory and the Department of Mechanical Engineering, Florida State University, Tallahassee, FL, USA, where he served as the Leader of the HTS Magnets and Materials Group. Under his leadership, the NHMFL-OST collaboration was the first to generate a magnetic field greater than 25 T with a superconducting magnet. In 2009, he joined North Carolina State University, Raleigh, NC, USA as the Head of the Department of Materials Science and Engineering and as the Kobe Steel Distinguished Professor. He has published more than 190 peer-reviewed journal articles and graduated 34 Ph.D. students, many of whom are now serving in leadership roles in the applied superconductivity community. His research interests include superconducting materials, with emphases on manufacturing-relevant processing techniques, performance-limiting mechanisms, and failure mechanisms.

Prof. Schwartz was the Editor-in-Chief of the IEEE TRANSACTIONS ON APPLIED SUPERCONDUCTIVITY from 2004 to 2012. He was the recipient of the Roger W. Boom Award from the Cryogenic Society of America in 1998 and is one of the youngest fellows in IEEE history.